Origin and Function of Myofibroblasts in Kidney Fibrosis

Valerie S. LeBleu, Gangadhar Taduri, Joyce O'Connell, Yingqi Teng, Vesselina G. Cooke, Craig Woda, Hikaru Sugimoto and Raghu Kalluri

Supplementary Figures and Figure Legends:

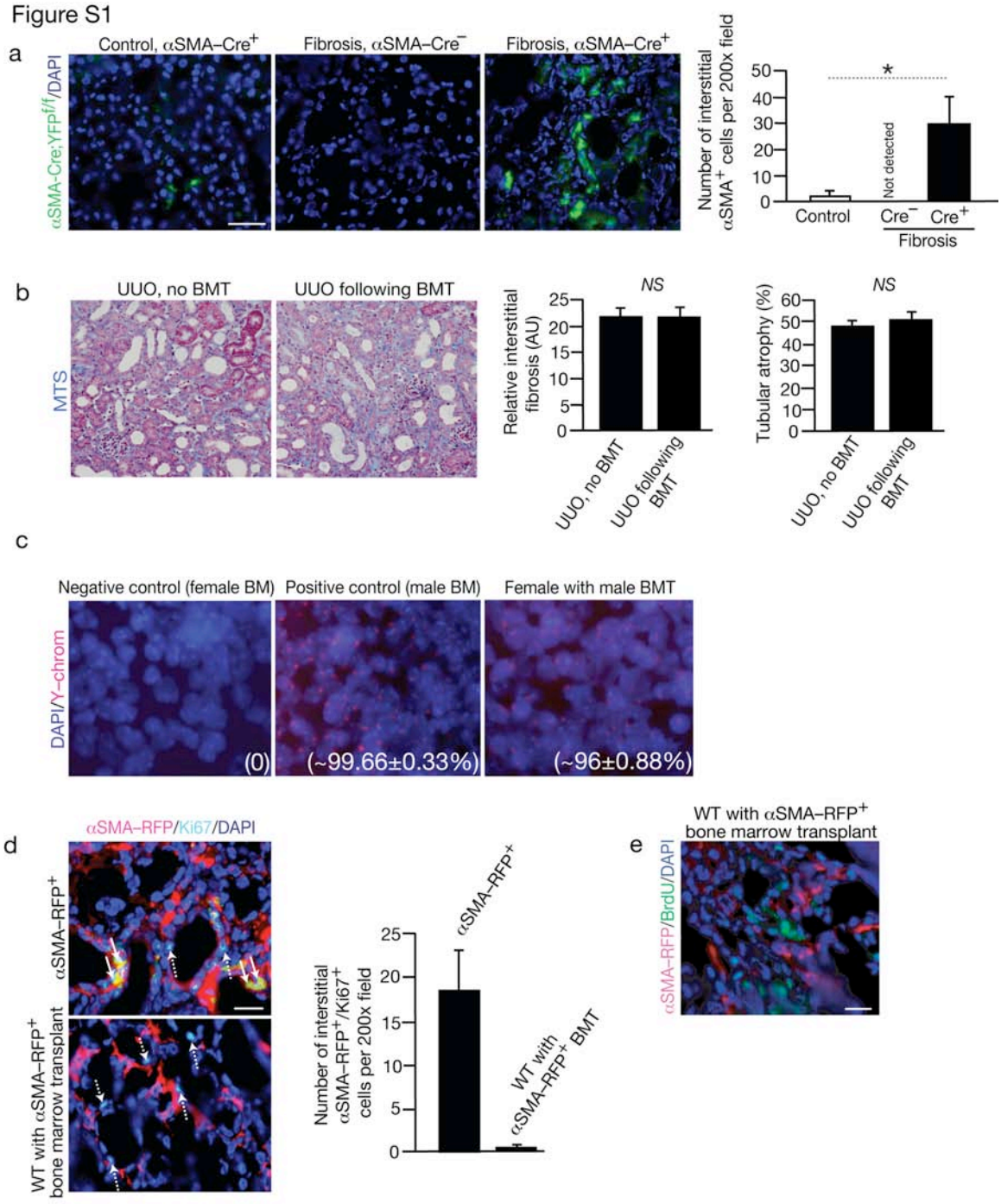

Figure S1. Linage tracing of αSMA$^+$ cells and bone marrow transplant supporting data

(**a**) Visualization of YFP$^+$ cells in non-fibrotic contralateral (Control) kidney of αSMA-Cre$^+$;YFP$^{f/f}$ mice, and fibrotic kidneys of αSMA-Cre$^+$;YFP$^{f/f}$ and αSMA-Cre$^-$;YFP $^{f/f}$ mice (used as negative control) 10 days post UUO. Graph depicts the quantitative analysis of YFP$^+$ cells per visual field in control and fibrotic kidney in αSMA-Cre$^+$;YFP$^{f/f}$ mice. (**b**) Representative Masson Trichrome staining (MTS) and morphometric analyses of kidneys of mice 10 days post UUO ('UUO, no BMT', *n* = 5) and of mice day 10 post UUO which received bone marrow transplant 4-5 weeks prior to UUO ('UUO following BMT'; *n* = 5). (**c**) Representative Y-chromosome FISH labeling of bone marrow cells cyto-spinned from female (*n* = 1), male (*n* = 1), and female mice transplanted with bone marrow from a male donor (*n* = 3). Percentages represent the relative number of Y-chromosome labeled nuclei. (**d**) Immunolabeling for Ki67 in fibrotic kidney of αSMA-RFP mice and WT mice transplanted with bone marrow from αSMA-RFP donor. Dashed arrows point to RFP$^-$/Ki67$^+$ cells and filled arrows point to RFP$^-$/Ki67$^+$ cells. Quantitation of αSMA-RFP$^+$/Ki67$^+$ myofibroblasts in fibrotic kidney. (**e**) Immunolabeling for BrdU in fibrotic kidney of αSMA-RFP mice and WT mice transplanted with bone marrow from αSMA-RFP donor (mice were euthanized 1-2 hours post BrdU injection). AU: Arbitrary Units. DAPI(blue): nuclei. Scale bar: 50 μm. Data is presented as mean ± s.e.m. *t*-test, **P* < 0.05, *NS*: not significant.

Figure S2

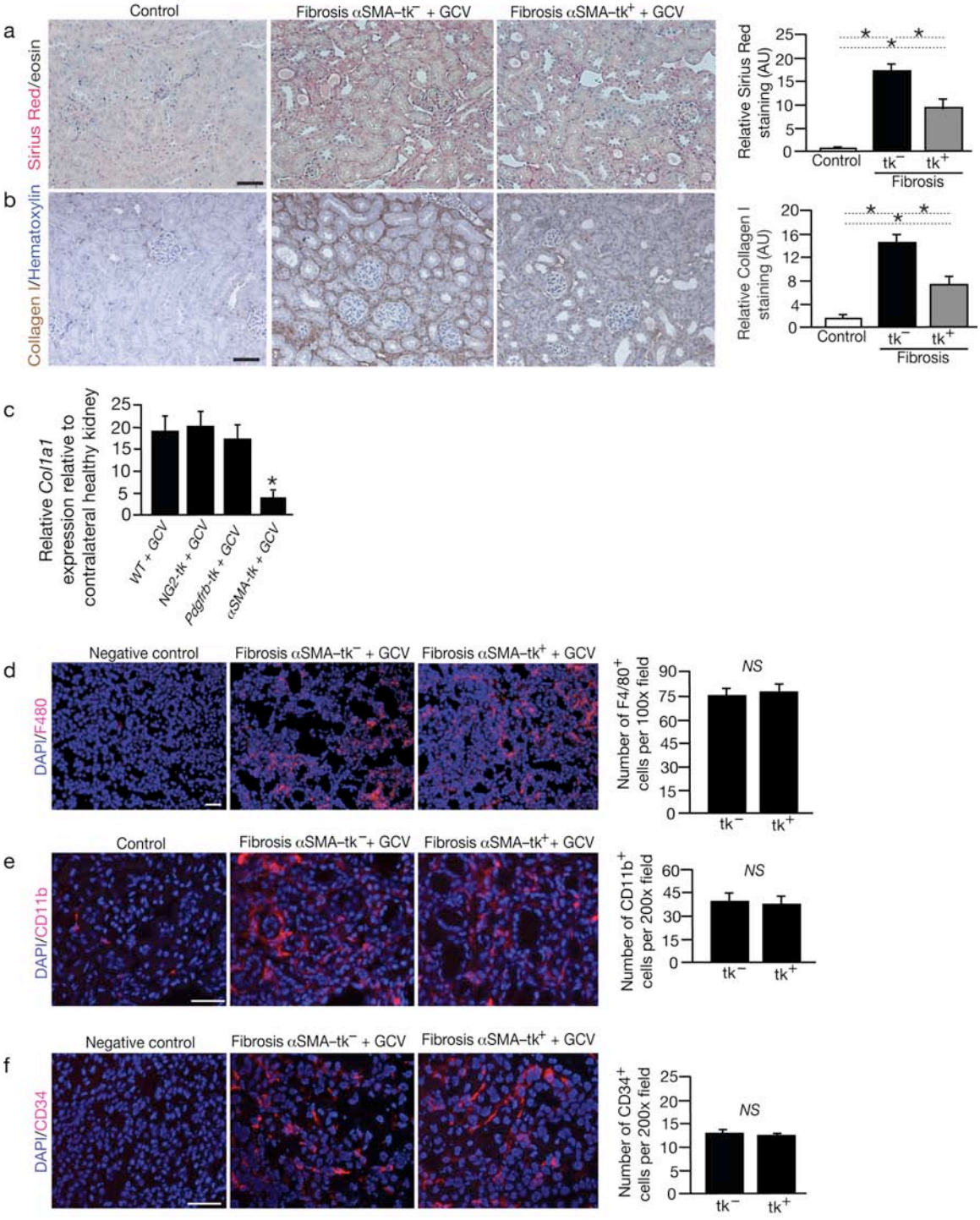
a
Control
Fibrosis αSMA–tk⁻ + GCV
Fibrosis αSMA–tk⁺ + GCV
Sirius Red/eosin
Relative Sirius Red staining (AU)
Control
tk⁻
tk⁺
Fibrosis
b
Collagen I/Hematoxylin
Relative Collagen I staining (AU)
c
Relative Col1a1 expression relative to contralateral healthy kidney
WT + GCV
NG2-tk + GCV
Pdgfrb-tk + GCV
αSMA-tk + GCV
d
Negative control
DAPI/F480
Number of F4/80⁺ cells per 100x field
NS
e
DAPI/CD11b
Number of CD11b⁺ cells per 200x field
f
DAPI/CD34
Number of CD34⁺ cells per 200x field

Figure S2. Supporting data for αSMA-tk ablation in UUO-induced renal fibrosis

(**a**) Representative Sirius Red staining of control (n=5), WT (n=5) and αSMA-tk$^+$ (n=5) fibrotic kidneys treated with GCV, and morphometric analysis for relative Sirius red labeling. (**b**) Representative type I collagen (Collagen I) immunolabeling of control, WT and αSMA-tk$^+$ fibrotic kidneys treated with GCV, and morphometric analysis for relative type I collagen staining. (**c**) Relative *Col1a1* expression by Q-PCR analysis in kidneys of indicated experimental groups, normalized to contralateral healthy kidneys. (**d**) Representative images and quantification of macrophage infiltration (F4/80$^+$) fibrotic kidney from αSMA-tk$^-$ and αSMA-tk$^+$ mice treated with GCV. (**e**) Representative images and quantification of macrophage infiltration (CD11b$^+$) fibrotic kidney from αSMA-tk$^-$ and αSMA-tk$^+$ mice treated with GCV. (**f**) Representative images and quantification of endothelial cells (CD34$^+$) fibrotic kidney from αSMA-tk$^-$ and αSMA-tk$^+$ mice treated with GCV. Negative control: secondary antibody only. Control: contralateral healthy kidney. AU: Arbitrary Units. DAPI(blue): nuclei. Scale bar: 50 μm. Data is presented as mean ± s.e.m. *t*-test, **P* < 0.05, *NS*: not significant.

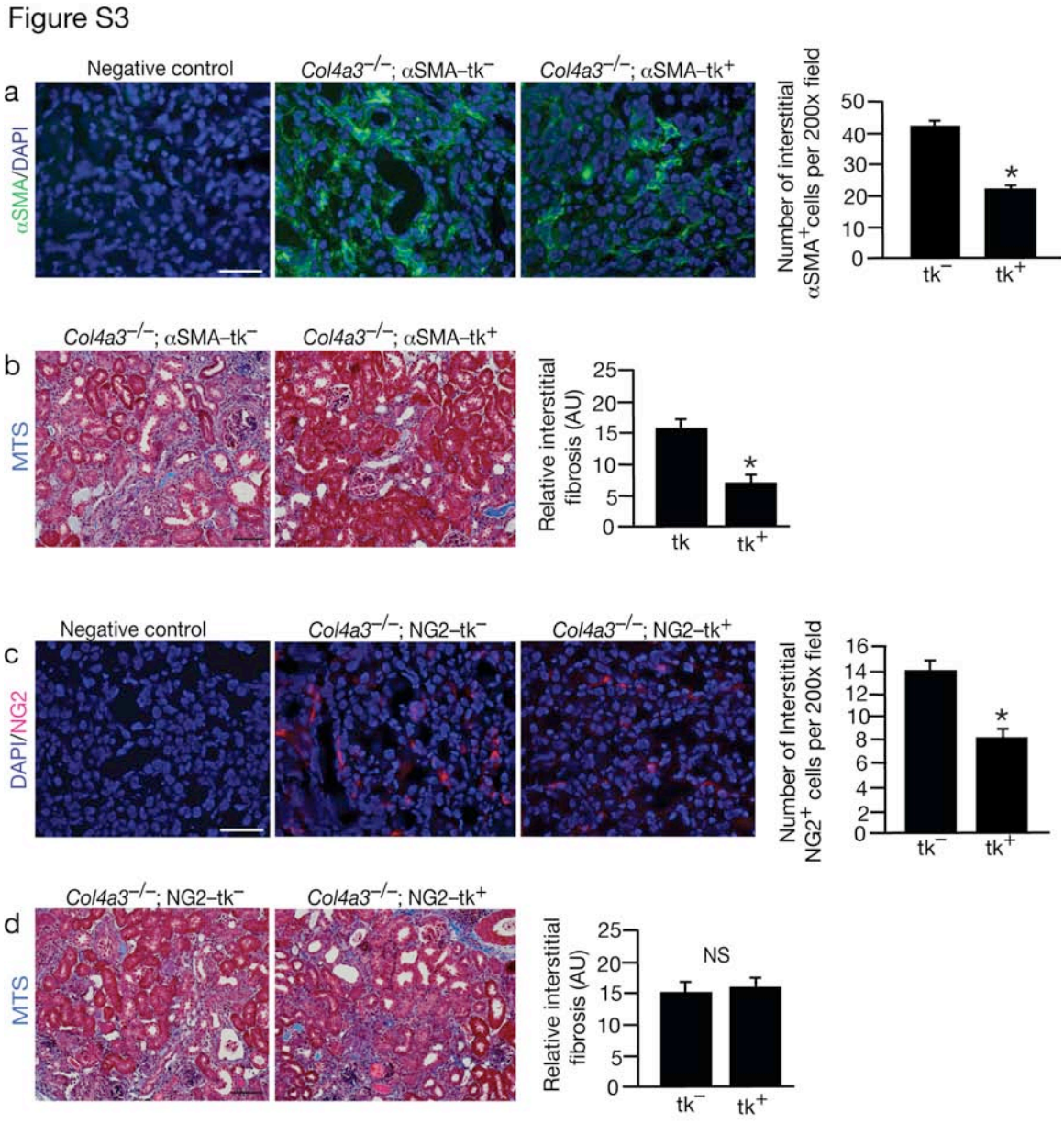

Figure S3. Ablation of αSMA$^+$ cells but not NG2$^+$ cells improves fibrosis in *Col4a3*$^{-/-}$ mice

(**a**) Immunolabeling for αSMA in fibrotic kidney of *Col4a3*$^{-/-}$;αSMA-tk$^-$ (n=5) and *Col4a3*$^{-/-}$;αSMA-tk$^+$ (n=5) mice treated with GCV and quantitation of αSMA$^+$ cells per field of view. (**b**) Representative Masson Trichrome staining (MTS) of

Col4a3$^{-/-}$;αSMA-tk^{-} and *Col4a3*$^{-/-}$;αSMA-tk^{+} mice treated with GCV and morphometric analysis for relative interstitial fibrosis. (**c**) Immunolabeling for NG2 in fibrotic kidney of *Col4a3*$^{-/-}$;NG2-tk^{-} (n=5) and *Col4a3*$^{-/-}$;NG2-tk^{+} (n=5) mice treated with GCV and quantitation of NG2^{+} cells per field of view. **D**. Representative Masson Trichrome (MTS) staining of *Col4a3*$^{-/-}$;NG2-tk^{-} and *Col4a3*$^{-/-}$;NG2-tk^{+} mice treated with GCV and morphometric analysis for relative interstitial fibrosis. Negative control, secondary antibody only. Control: contralateral healthy kidney. AU: Arbitrary Units. DAPI(blue): nuclei. Scale bar: 50μm. Data is presented as mean ± s.e.m. *t*-test, **P* < 0.05, *NS*: not significant.

Figure S4

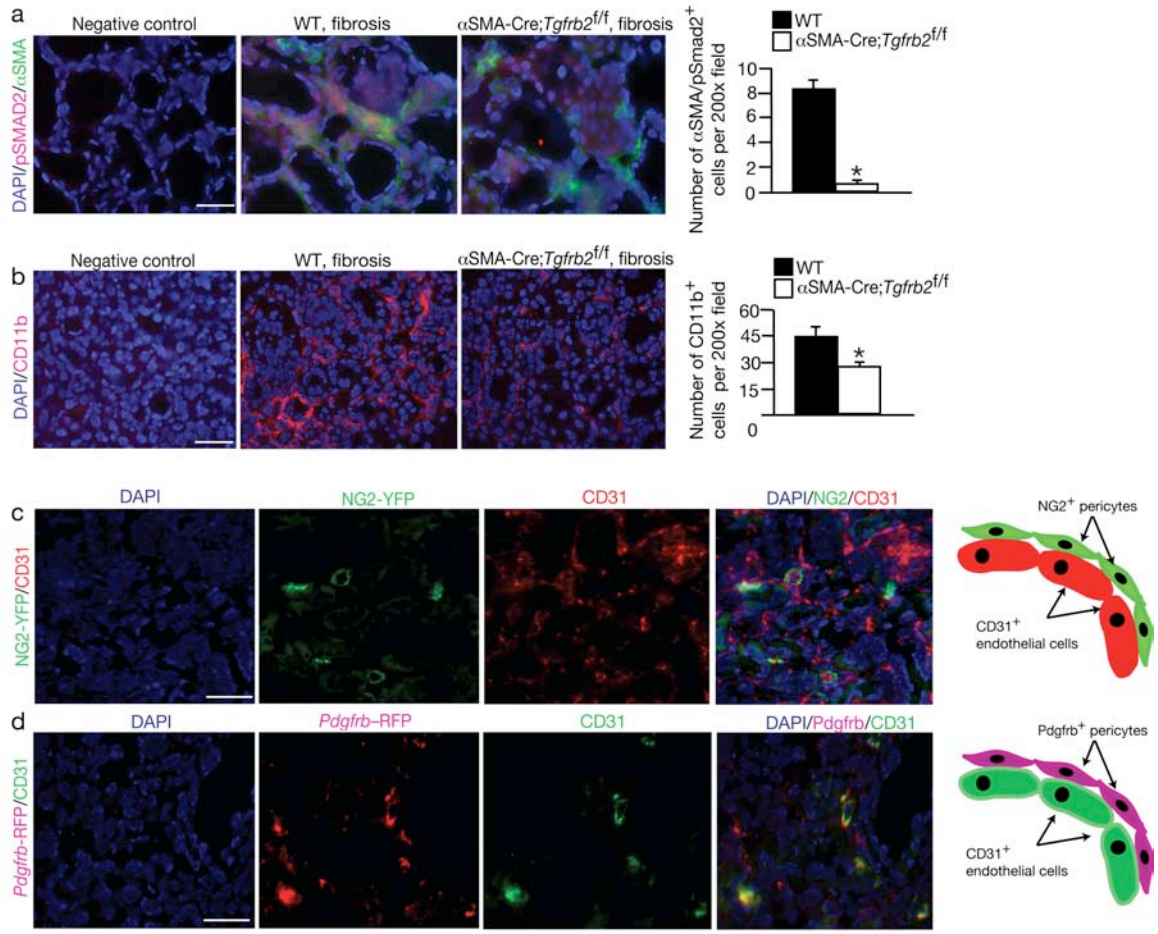

Figure S4. **Supporting data for αSMA-Cre;Tgfrb2$^{f/f}$ mice and NG2-YFP and *Pdgfrb*-RFP visualization in normal kidney.**

(**a**) Immunolabeling for phosphorylated Smad2 (pSmad2) and αSMA in WT and αSMA-Cre;Tgfrb2$^{f/f}$ fibrotic kidneys. Graph depicts quantitation of αSMA/pSmad2 double positive cells per field of view. (**b**) Immunolabeling for CD11b^{+} macrophages in WT and αSMA-Cre;Tgfrb2$^{f/f}$ fibrotic kidneys. Graph depicts quantitation of CD11b^{+} macrophages per field of view. (**c**) Representative immunofluorescent images showing YFP expression (from NG2-YFP^{+} cells) and

CD31 immunolabeling (endothelial cells) in mouse kidneys and schematic representation of results: $NG2^+$ pericytes are noted on the abluminal side of the vessel. (**d**) Representative immunofluorescent images showing RFP expression (from *Pdgfrb*-RFP^+ cells) and CD31 immunolabeling (endothelial cells) in mouse kidneys and schematic representation of results: $Pdgfrb^+$ pericytes are noted on the abluminal side of the vessel. DAPI(blue): nuclei. Scale bar: 50 μm. Data is presented as mean ± s.e.m. *t*-test, $*P < 0.05$.

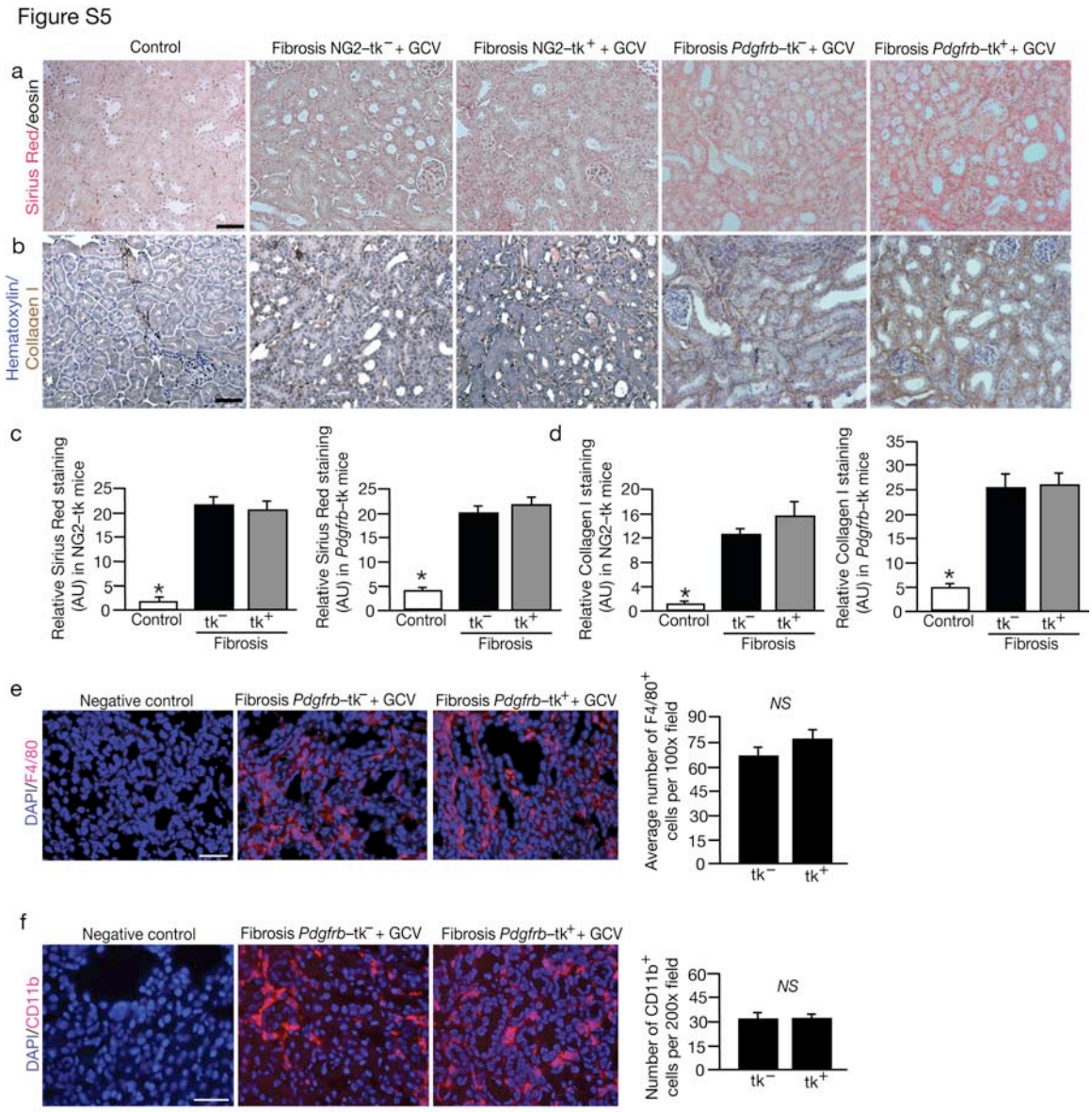

Figure S5. Pericytes do not functionally contribute to fibrosis

(**a**-**b**) Representative Sirius red (**a**), and type I collagen staining (**b**) of non-fibrotic contralateral (Control) kidney, and fibrotic kidneys from NG2-tk^{-}, NG2-tk^{+}, *Pdgfrb*-tk^{-} and *Pdgfrb*-tk^{+} mice treated with GCV. (**c**-**d**) Morphometric analysis for relative Sirius red staining (**c**), and type I collagen staining (**d**) of indicated

experimental groups. (**e**) Representative images and quantification of macrophage infiltration ($F4/80^+$) in fibrotic kidney from *Pdgfrb*-tk^- and *Pdgfrb*-tk^+ mice treated with GCV. (**f**) Representative images and quantification of macrophage infiltration ($CD11b^+$) fibrotic kidney from *Pdgfrb*-tk^- and *Pdgfrb*-tk^+ mice treated with GCV. Negative control: secondary antibody only. DAPI(blue): nuclei. AU: Arbitrary Units. Scale bar: 50 μm. Data is presented as mean ± s.e.m. *t*-test, $*P < 0.05$, *NS*: not significant.

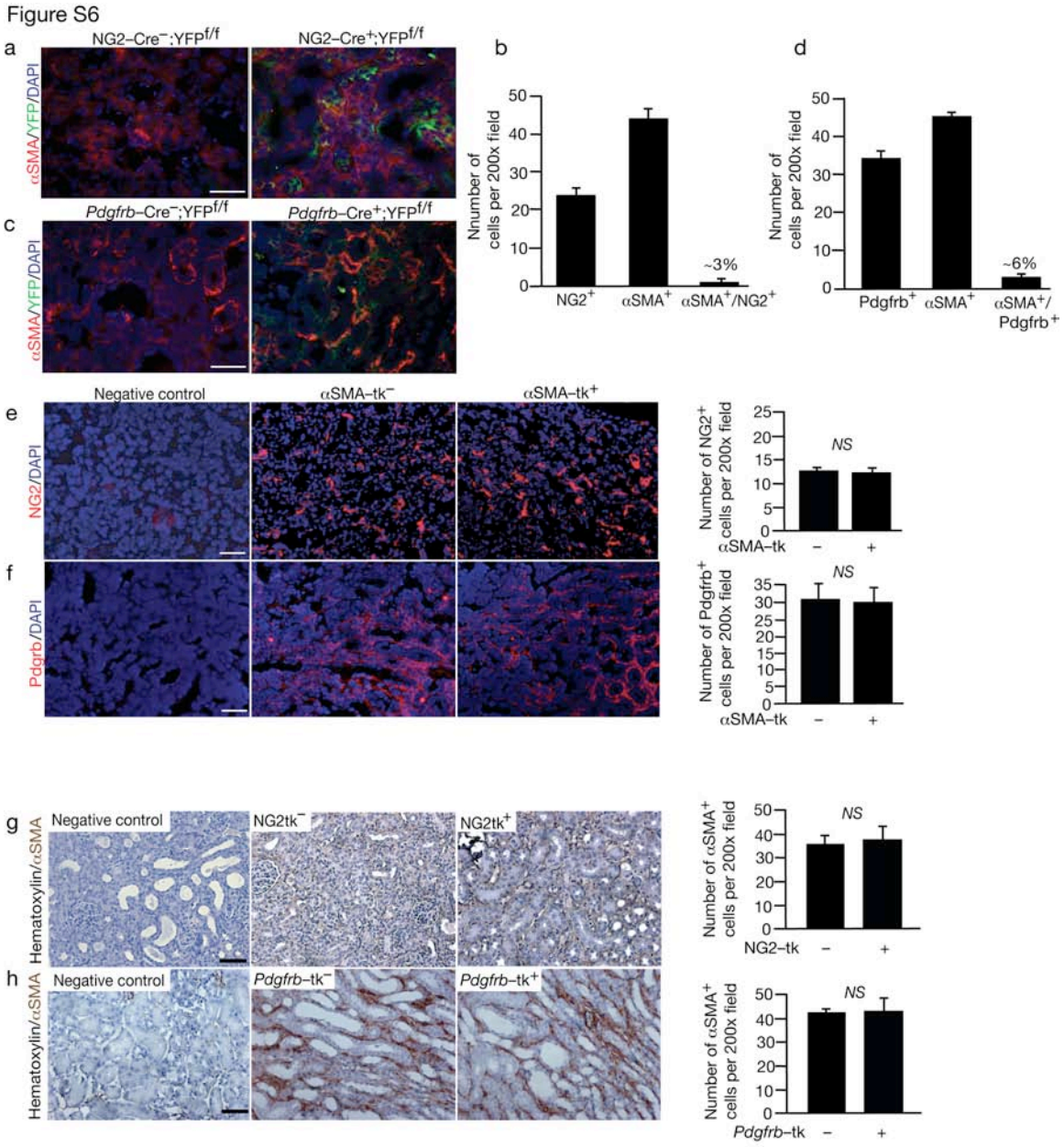

Figure S6. αSMA⁺ myofibroblasts in the fibrotic kidney emerge independently of the vascular pericyte lineage

(**a**) αSMA immunolabeling of kidneys in lineage tagged NG2-Cre;YFP$^{f/f}$ mice, UUO fibrotic kidney (*n* = 5). (**b**) Relative number of αSMA^{+}, NG2^{+}, and αSMA^{+}/NG2^{+} (double positive) cells per field of view in NG2-Cre+;YFP$^{f/f}$ fibrotic kidney. On average 3% of αSMA/NG2 double positive cells were detected. (**c**)

αSMA immunolabeling of kidneys in lineage tagged *Pdgfrb*-Cre;YFP$^{f/f}$ mice. (**d**) Relative number of αSMA^{+}, Pdgfrb^{+}, and αSMA^{+}/Pdgfrb^{+} (double positive) cells per field of view in *Pdgfrb*-Cre^{+};YFP$^{f/f}$ fibrotic kidney. On average 6% of αSMA/Pdgfrb double positive cells were detected. (**e**) NG2 immunolabeling of fibrotic kidney from αSMA-tk^{-} and αSMA-tk^{+} mice treated with GCV and number of NG2^{+} cells per visual field in αSMA-tk^{-} and αSMA-tk^{+} fibrotic kidneys. (**f**) Pdgfrb immunolabeling of fibrotic kidney from αSMA-tk^{-} and αSMA-tk^{+} mice treated with GCV and number of Pdgfrb^{+} cells per visual field in αSMA-tk^{-} and αSMA-tk^{+} fibrotic kidneys. (**g**) αSMA immunolabeling of fibrotic kidney from NG2-tk^{-} and NG2-tk^{+} mice treated with GCV and number of αSMA^{+} cells per visual field in NG2-tk^{-} and NG2-tk^{+} fibrotic kidneys. (**h**) αSMA immunolabeling of fibrotic kidney from *Pdgfrb*-tk^{-} and *Pdgfrb*-tk^{+} mice treated with GCV and number of αSMA^{+} cells per visual field in *Pdgfrb*-tk^{-} and *Pdgfrb*-tk^{+} fibrotic kidneys. Negative control: secondary antibody only. DAPI(blue): nuclei. Scale bar: 50 μm. Data is presented as mean ± s.e.m. *t*-test, *NS*: not significant.

Supplementary Methods:

Primer sequence:

Mouse *Col1a1*	5'-GCTCCTCTTAGGGGCCACT-3' 5'-CCACGTCTCACCATTGGGG-3'
Mouse *Acta2* (αSMA)	5'-CCAGTTGTACGTCCAGAGGC-3' 5'-GGTGATGATGTCCCAGGGC-3'
Mouse *β-actin*	5'-GGCTGTATTCCCCTCCATCG-3' 5'-CCAGTTGGTAACAATGCCATGT-3'

Generation of αSMA-Cre mice

A fragment of the cre recombinase gene with 3' UTR was amplified from plasmid p705-Cre (Gene Bridge GmbH, Germany) using the following primers: 5' ATGTCCAATTTACTGACCGTACACC 3' (Forward); 5' CTAATCGCCATCTTCCAGCAGGC 3' (Reverse). The extended αSMA (*Acta2*) promoter (described above) was cloned into the pCR2.1-TOPO vector (Invitrogen) using EcoRI and NotI restriction sites, then this αSMA promoter-TOPO construct and the cre fragment were digested and ligated together. The whole αSMA-Cre construct was released from the vector using SpeI and XbaI before purification and injection into fertilized eggs. The transgenic mice were generated in the Brigham and Women's Hospital Transgenic Core Facility (Boston, MA) on a FVB background and backcrossed at least 10 generations to a BALB/c background. To characterize the specificity of the αSMA-Cre mice, we crossed these mice with R26R-LoxP-Stop-LoxP-YFP mice. In normal kidney, such fate mapping analysis revealed that αSMA-Cre activity is largely undetected. However, some rare positive areas associated with large blood vessel walls and occasional renal epithelial tubules are observed in all mice. In

the fibrosis setting, the αSMA-Cre activity was predominantly seen in renal interstitial cells, some renal tubular epithelial cells and occasional blood vessels.

Generation of αSMA-tk mice

A truncated version of the herpes simplex 1 virus thymidine kinase (HSV1-tk) gene with 3' UTR was amplified from plasmid fsp1-TK[1] using the following primers: 5' ATGCCCACGCTACTGCGGG 3' (Forward); 5' GTGGATAACCGTATTACCGCC 3' (Reverse). The extended αSMA promoter was cloned into the pCR2.1-TOPO vector (Invitrogen) using EcoRI and NotI restriction sites, then this αSMA promoter-TOPO construct and the tk fragment were digested and ligated together. The whole αSMA-tk construct was released from the vector using EcoRI and XbaI before purification and injection into fertilized eggs. The transgenic mice were generated in the Brigham and Women's Hospital Transgenic Core Facility (Boston, MA) on a FVB background and backcrossed at least 10 generations to a BALB/c genetic background.

Generation of NG2-Cre mice

Genomic DNA (~5 kb) containing the NG2 (*Cspg4*) promoter and part of NG2 exon 1 was amplified by PCR and a SfiI restriction site was introduced into the reverse primer. The start codon ATG was mutated in the reverse primer (C to A). The PCR product was TA-cloned into the pCR2.1-TOPO vector (Invitrogen). The NG2 promoter was then excised using EcoRI and inserted into p705-Cre vector (Gene Bridge GmbH, Germany). The resulting NG2-Cre construct was released

from the TOPO vector using SfiI and NheI, purified and injected into fertilized eggs (FVB) to generate NG2-Cre transgenic mice. NG2-Cre mice were backcrossed for at least 10 generations to a BALB/c genetic background. To characterize the specificity of the NG2-Cre mice, we crossed these mice with R26R-LoxP-Stop-LoxP-YFP mice. In normal kidney, such fate mapping analysis revealed that NG2-Cre activity is largely restricted to large and small vascular structures including the glomeruli. In the fibrosis setting, the NG2-Cre activity was seen in renal interstitial cells and vascular structures of the kidney.

Supplemental Reference:

1. Iwano, M.*, et al.* Conditional abatement of tissue fibrosis using nucleoside analogs to selectively corrupt DNA replication in transgenic fibroblasts. *Mol Ther* **3**, 149-159 (2001).